

Article

Reevaluation of the K/Rb-Li Systematics in Muscovite as a Potential Exploration Tool for Identifying Li Mineralization in Granitic Pegmatites

Michael A. Wise¹, Adam C. Curry²  and Russell S. Harmon^{2,*} 

¹ Department of Mineral Sciences, National Museum of Natural History, Smithsonian Institution, Washington, DC 20560, USA; wisem@si.edu

² Department of Marine, Earth, and Atmospheric Sciences, North Carolina State University, Raleigh, NC 27695, USA; accurry3@ncsu.edu

* Correspondence: rsharmon@ncsu.edu

Abstract: A dataset of >1190 published compositional analyses of muscovite from granitic pegmatites of varying mineralogical types was compiled to reevaluate the usefulness of K-Rb-Li systematics of muscovite as a tool for distinguishing mineralogically simple pegmatites from pegmatites with potential Li mineralization. Muscovite from (i) common, (ii) (Be-Nb-Ta-P)-enriched, (iii) Li-enriched, and (iv) REE- to F-enriched pegmatites contain Li contents that vary between 10 and 20,000 ppm depending on the degree of pegmatite fractionation. Common pegmatites are characterized by low degrees of fractionation as exhibited by K/Rb ratios ranging from 618 and 25 and Li contents generally being <200 ppm but infrequently as high as 743 ppm in muscovite. Moderately fractionated pegmatites with Be, Nb, Ta, and P enrichment contain muscovite having K/Rb ratios mostly between 45 and 7 plus Li contents between 5 to >1700 ppm. Muscovite from moderately to highly fractionated Li-rich pegmatites exhibit a wide range of K/Rb ratios and Li values: (i) K/Rb = 84 to 1.4 and Li = 35 to >18,100 ppm for spodumene pegmatites, (ii) K/Rb = 139 to 2 and Li = 139 to >18,500 ppm for petalite pegmatites, and (iii) K/Rb = 55 to 1.5 and Li = 743 to >17,800 ppm for lepidolite pegmatites. Pegmatites that host substantial REE- and F-rich minerals may carry muscovite with K/Rb ratios between 691 to 4 that has Li contents between 19 to 15,690 ppm. The K/Rb-Li behavior of muscovite can be useful in assessing the potential for Li mineralization in certain granitic pegmatite types. The proposed limits of K/Rb values and Li concentrations for identifying spodumene- or petalite-bearing pegmatites as part of an exploration program is reliable for Group 1 (LCT) pegmatite populations derived from S-type parental granites or anatexitic melting of peraluminous metasedimentary rocks. However, it is not recommended for application to Group 2 (NYF) pegmatites affiliated with anorogenic to post-orogenic granitoids with A-type geochemical signatures or that derived by the anatexis of mafic rocks that generated REE- and F-rich melts.

Keywords: muscovite; lithium; K/Rb; granitic pegmatites; laser-ablation inductively coupled plasma mass spectrometry (LA-ICP-MS); laser-induced breakdown spectroscopy (LIBS)



Citation: Wise, M.A.; Curry, A.C.; Harmon, R.S. Reevaluation of the K/Rb-Li Systematics in Muscovite as a Potential Exploration Tool for Identifying Li Mineralization in Granitic Pegmatites. *Minerals* **2024**, *14*, 117. <https://doi.org/10.3390/min14010117>

Academic Editors: David Lentz, Victoria Maneta, Mona-Liza C. Sirbescu and Julian Menuge

Received: 27 October 2023

Revised: 17 January 2024

Accepted: 20 January 2024

Published: 22 January 2024



Copyright: © 2024 by the authors. Licensee MDPI, Basel, Switzerland. This article is an open access article distributed under the terms and conditions of the Creative Commons Attribution (CC BY) license (<https://creativecommons.org/licenses/by/4.0/>).

1. Introduction

Critical minerals are natural materials essential to the welfare of global economies and the transition to a 'green' future. The transition to clean energy technologies, for example, is helping to stimulate an unprecedented demand for lithium, an element that is indispensable in the electric vehicle and lithium-ion battery markets in addition to its more conventional use in the glass and ceramics industries. While the main global source of lithium continues to be lithium brines (salars), granitic pegmatites are also being exploited as a complementary lithium source and one that is likely to dominate in the future. Most granitic pegmatites do not contain economic concentrations of Li; however, pegmatite melts that have undergone considerable rare-element fractionation may develop

Li mineralization characterized by the presence of the lithium aluminosilicates spodumene, petalite, or lepidolite. Exploration programs designed to locate and identify granitic pegmatites that have potentially economic concentrations of Li can be time consuming and expensive. A typical approach to finding Li-enriched pegmatites involves extensive field work and sampling of non-lithium minerals, such as K-feldspar and muscovite, which are used as proxies for assessing the chemical evolution and rare-element enrichment of a pegmatite [1,2]. The trace element composition of muscovite is a particularly useful pathfinder in pegmatite exploration programs as a means of targeting potentially Li-rich pegmatite bodies [3,4].

Muscovite is the most important mica species present in granitic pegmatites and it is often the next most abundant mineral after quartz and feldspars. Muscovite crystallizes in many different pegmatite types and during many stages of pegmatite development. Wise et al. [5] proposed a pegmatite classification scheme that distinguishes three groups encompassing a broad spectrum of pegmatite types based on their assemblage of primary accessory rock-forming and rare-element minerals. Group 1 pegmatites are characterized by enrichment in Li, Rb, Cs, Be, Sn, Nb, Ta, B, P, and F but typically have low contents of Ti, Zr, Y, and REE. These pegmatites are analogous to the LCT family of Černý and Ercit [6]. The Group 2 pegmatites have a geochemical signature comparable to the NYF pegmatites of Černý and Ercit [6] that are characterized by their high abundances of Ga, Zr, Y, Nb, Ti, U, Th, REEs, Zn, F, and Cl. Group 3 pegmatites have no equivalent in the Černý and Ercit [6] classification scheme and are dominated by Al-, B-, and Be-rich accessory minerals. Muscovite occurs as a primary major to the minor phase in all three pegmatite groups but is generally more common in Group 1 pegmatites and, therefore, has received greater attention compared to muscovite from the other groups.

The complex crystallization history of granitic pegmatites typically leads to a wide range of textural features that often include muscovite as an integral component. Textural varieties, known from simple to highly fractionated rare-element pegmatites, include (i) quartz-muscovite aggregates typical of wall zones, (ii) medium- to coarse-grained 'books' of muscovite that occur in large masses or veins in intermediate zones and core margins, (iii) fine-grained silver to pale brown flakes of muscovite within aplitic or late-stage replacement and greisenized units, and (iv) greenish zoned muscovite crystals rimmed by lilac-colored Li-enriched muscovite found along the margins of miarolitic cavities.

The trace element character of muscovite from granitic pegmatites has been extensively studied and the behavior of Li, Rb, and Cs has proven extremely valuable in understanding the chemical evolution of pegmatites [1,3,7,8]. Muscovite trace element chemistry has also been used in exploration programs designed to identify mineralized pegmatite deposits. The K/Rb ratio and rare alkalis abundance of muscovite is often considered an important tool in the search for spodumene- or petalite-bearing pegmatites. Evaluating the Li potential of individual pegmatite bodies or pegmatite fields often utilizes the K/Rb-Li systematics of muscovite to differentiate unmineralized pegmatites from those carrying Li mineralization.

As reported by Černý and Burt [9], investigations of granitic pegmatites by Gordiyenko [10] showed that muscovite with Li contents of approximately 400 to 2000 ppm and K/Rb ratios < 25 were typical of spodumene-bearing pegmatites. Maneta and Baker [4] observed that Li concentrations exceeding 500 ppm in muscovite reliably indicated the presence of Li-aluminosilicate minerals in the Moblan pegmatites of Quebec, Canada. Selway et al. [2] suggested that pegmatites with the greatest potential for spodumene mineralization contain coarse-grained green muscovite with >2000 ppm Li and K/Rb ratios < 20. In a study of pegmatites from the former USSR, Gordiyenko [11] observed Li contents of 470 to 1370 ppm in muscovite from spodumene-bearing pegmatites. However, he concluded that these values could not differentiate spodumene-bearing pegmatites from non-spodumene-bearing pegmatites. Similarly, Smeds [12] examined the chemistry of muscovite from several Swedish pegmatites and identified three groups based on the K/Rb ratios and Li content: (i) muscovite with low K/Rb and high Li content from spodumene-bearing pegmatites, (ii) muscovite with intermediate K/Rb ratios and Li contents from pegmatites

where triphylite is the only Li-mineral present, and (iii) muscovite with high K/Rb ratios and high Li contents from pegmatites with no Li mineralization.

Based on these contradictory studies, there does not appear to be a clear consensus on the reliability of muscovite Li content as a viable tool for the prospecting and exploration for Li-rich pegmatites. To better understand the K/Rb-Li systematics of muscovite in granitic pegmatites and further assess its potential as an exploration tool, >1190 published analyses from 224 pegmatite localities served as the basis for this study. The localities selected for this study included (i) representatives of the global distribution of granitic pegmatites, (ii) both famous and obscure pegmatites, and (iii) historically and recently well-described economically and non-economically important deposits. This broad sampling of published data was necessary to ensure that a diverse range of pegmatite types were represented with the larger goal of minimizing bias in the dataset that could have arisen from the selection of only a few well-known localities. The muscovite data, presented in Tables 1–5, were assembled from a wide range of mineralogically and chemically diverse pegmatites largely from the Group 1 (LCT) affiliation, although some muscovite data from Group 2 (NYF) pegmatite were included for comparison. Additionally, we have also included LA-ICP-MS and LIBS analyses conducted on our own muscovite samples from select pegmatites for comparison to the published data. In all instances, only analyses of coarse- to medium-grained, presumably primary muscovite, were used in this study.

1.1. Characteristics of Group 1 (LCT) Pegmatites

The localities used for this study included Group 1 or LCT-type pegmatites as defined by Wise et al. [5] and Černý and Ercit [6], respectively. Published muscovite analyses were chosen from mineralogically simple and geochemically primitive common pegmatites to evolved pegmatites that includes representatives of the beryl ± columbite ± phosphate, spodumene, petalite, and lepidolite subtypes of Černý and Ercit [6]. Common pegmatites consist of essential rock-forming K-feldspar, quartz, albite, and muscovite with subordinate to accessory schorl, almandine, and biotite; beryl rarely occurs. Common pegmatites are often structurally unzoned to poorly zoned bodies and typically lack metasomatic replacement units. These pegmatites represent the least fractionated examples of all pegmatites used in this study. Pegmatites highlighted by beryl ± columbite ± phosphate assemblages often display distinct well-developed internal zonation with incipient metasomatic albite-rich or muscovite-rich greisen-like units. While accessory schorl, almandine, and apatite are common, assemblages containing minor to subordinate columbite-group minerals and the primary accessory phosphates graffonite-beusite, sarcopside, triphylite-lithiophilite, and amblygonite-montebrazite underscore the modest rare-element enrichment and chemically evolved nature of the pegmatites.

The most widespread type of Li-rich pegmatite is characterized by having spodumene as the dominant Li-aluminosilicate mineral. Most spodumene-bearing pegmatites have a magmatic mineral assemblage of quartz, K-feldspar, albite, and muscovite. They are normally very coarse-grained and exhibit well-developed complex internal zoning that often is disrupted by extensive albitization and ‘greisenization’. In general, these pegmatites frequently contain some zones richer in K-feldspar relative to albite. By comparison, albite-spodumene subtype pegmatites are finer-grained texturally with nearly homogeneous internal structure and bulk compositions, with albite and quartz dominant over K-feldspar. Subtle textural internal zoning occurs in the form of minor layered albitic assemblages, lenses of randomly oriented blocky quartz-feldspar, and features of sub-perpendicular to obliquely oriented lath-shaped crystals of spodumene and K-feldspar. Rare-element mineralization for both spodumene-bearing types may include beryl, columbite-group minerals, and cassiterite, while lepidolite, pollucite, and elbaite are less common in the albite-spodumene variety.

Li-rich pegmatites in which muscovite is extremely scarce include the lepidolite and elbaite subtypes of Černý and Ercit [6]. Lepidolite pegmatites have lepidolite as the dominant Li-bearing mineral [6]. They are distinctly zoned with typically massive fine-

to medium-grained lepidolite-rich zones or units that occur within the innermost portion of the pegmatite. Minor accessory minerals may include spessartine-almandine, beryl, cassiterite, columbite-group minerals, elbaite-rossmanite, topaz, apatite, zircon, microlite-subgroup minerals, and rare amblygonite-montebrazite, petalite, or spodumene. Conversely, elbaite subtype pegmatites carry elbaite as the only substantial Li-bearing mineral [13]. Elbaite pegmatites also display well-developed internal zonation and tend to host significant proportions of miarolitic cavities (i.e., pockets) in the central zones of the pegmatite. The conspicuous presence of Mn-rich elbaite, abundance of spessartine, and general scarcity of micas and topaz along with the rare occurrence of other B-rich minerals, such as hambergite and danburite, highlight some of the mineral assemblages found in elbaite-subtype pegmatites.

The occurrence of coarse-grained primary petalite as a dominant Li-bearing mineral in granitic pegmatites suggests crystallization at low pressures (approximately 1.5 to 3 kilobars) compared to spodumene which is stable at higher pressures of 3 to 5 kilobars. In some pegmatites, pressure-temperature conditions may exist where primary petalite becomes unstable and breaks down to a fine-grained intergrowth of spodumene and quartz, known as 'squi'. Consequently, spodumene + quartz pseudomorphs after petalite have often been used to infer pressure-temperature conditions during pegmatite crystallization.

Granitic pegmatites where petalite occurs as the prominent Li-bearing mineral generally display well-developed internal zonation and is oftentimes intensely metasomatized. Chemically, petalite-bearing pegmatites show extreme enrichment in Li, Rb, Cs, Ta, Sn, Be, B, and F. Subsequently, rare-element mineralization in these pegmatites may include pollucite, lithian muscovite, lepidolite, beryl, columbite-group minerals, cassiterite, tapiolite-(Fe), wodginite, amblygonite, and triphylite.

1.2. Characteristics of Group 2 (NYF) Pegmatites

The occurrence of muscovite in Group 2 pegmatites is extremely limited compared to Group 1 pegmatites. Muscovite analyses available for this study represent poorly zoned to well-zoned pegmatites described as (i) amazonite-bearing pegmatites that may carry accessory zircon, fluorite, topaz, columbite-(Fe), and cassiterite, (ii) pegmatites with notable quantities of rare-earth minerals such as allanite-(Ce), samarskite-(Y), gadolinite-(Ce), gadolinite-(Y), fergusonite-(Y), monazite-(Ce), and REE-enriched fluorite, and (iii) pegmatites characterized by substantial Be mineralization (beryl or phenakite) accompanied by subordinate to local enrichment in F (topaz and fluorite), B (schorl), and Nb-Ta (columbite-tantalite, euxenite) mineralization. Lithium mineralization in Group 2 (NYF) pegmatites is uncommon but, when present, typically occurs as the Li-enriched micas, zinnwaldite, and ferroan lepidolite, rather than as spodumene or petalite.

1.3. Metasomatic Alteration in Pegmatites

The vast majority of granitic pegmatites do not show evidence of pervasive metasomatic alteration or replacement within or outside of the pegmatite body. When present, metasomatic effects may be manifested by the selective replacement of individual mineral species through to the nearly complete replacement of primary assemblages in pre-existing pegmatite zones or units. Metasomatic alteration of primary silicates, oxides, and phosphates can result in the formation of a number of secondary phases (e.g., fine-grained muscovite after microcline or topaz, albite, and muscovite assemblages after spodumene). Metasomatism can cause localized albitization and 'greisenization' in moderately to highly fractionated pegmatites resulting in the formation of massive units of saccharoidal (sugary-textured) albite or massive units of very fine to fine-grained lithium-enriched micas that develop from assemblages with K-feldspar and/or lithium aluminosilicates [14]. The texture of 'greisen'-like muscovite formed by metasomatic processes is generally as dense masses of very fine- to fine-grained scales compared to coarse-grained primary 'book' muscovite.

2. Analytical Methods

2.1. Laser Ablation Inductively-Coupled Plasma Mass Spectrometry

Laser ablation inductively-coupled plasma mass spectrometry (LA-ICP-MS) for muscovite trace element contents was performed at the LionChron facility at the Pennsylvania State University (University Park, PA, USA). Samples were mounted in epoxy and ablated using a Analyte G2 excimer laser ablation system (Teledyne, Bozeman, MT, USA) with a HeEx2 ablation cell, coupled to a Thermo Scientific iCAP-RQ ICPMS system (Thermo Scientific, Waltham, MA, USA) for trace elements. The total Ar gas flow for the experiment was 1 L/min, with total He gas flows from the laser at 0.44 L/min. All samples were run in back-to-back sessions, with an 85 μm spot, 10 Hz repetition rate, 180 shots, and a laser fluence at the sample surface of 3.66 J/cm², yielding pit depths in the order of ~ 10 μm . The laser was first fired three times with the same spot size to remove surface contamination and this material was allowed to wash out for ~ 15 s. Analyses of unknowns were bracketed by analyses of trace-element glass NIST612 [15] and whole-rock glasses from the Max-Planck-Institut [16] spanning a range of compositions, including Gorgona Island komatiite G132-G, Kilauea basalt KL2-G, Mauna Loa basalt ML3B-G, Alpine quartz diorite T1G, Mt. St. Helens andesite StHs6/80-G, and Icelandic rhyolite ATHO-G. KL2-G was used as the primary reference material for all analyses, except for TI for which no KL2-G data exist, and thus was reduced with NIST612 as the primary standard. For trace-element quantification, ²⁷Al (using data collected from prior EPMA sessions on the same grains) was used as an internal standard, with measured peaks on the iCAP-RQ at ⁷Li, ⁹Be, ²³Na, ²⁴Mg, ²⁷Al, ²⁹Si, ³¹P, ⁴⁴Ca, ⁴⁵Sc, ⁴⁹Ti, ⁵¹V, ⁵²Cr, ⁵⁵Mn, ⁵⁹Co, ⁶⁰Ni, ⁶³Cu, ⁶⁶Zn, ⁷¹Ga, ⁷³Ge, ⁷⁵As, ⁷⁷Se, ⁸⁵Rb, ⁸⁸Sr, ⁸⁹Y, ⁹⁰Zr, ⁹³Nb, ⁹⁵Mo, ¹¹¹Cd, ¹¹⁵In, ¹¹⁸Sn, ¹²¹Sb, ¹³³Cs, ¹³⁷Ba, ¹³⁹La, ¹⁴⁰Ce, ¹⁴¹Pr, ¹⁴⁶Nd, ¹⁴⁷Sm, ¹⁵³Eu, ¹⁵⁷Gd, ¹⁵⁹Tb, ¹⁶³Dy, ¹⁶⁵Ho, ¹⁶⁶Er, ¹⁶⁹Tm, ¹⁷²Yb, ¹⁷⁵Lu, ¹⁷⁸Hf, ¹⁸¹Ta, ¹⁸²W, ²⁰⁵Tl, ²⁰⁸Pb, ²⁰⁹Bi, ²³²Th, and ²³⁸U. Iolite version 4 [17] was used to correct measured isotopic ratios and elemental intensities for baselines, time-dependent laser-induced inter-element fractionation, plasma-induced fractionation, and instrumental drift. The mean and standard error of the measured ratios of the backgrounds and peaks were calculated after the rejection of outliers more than two standard errors beyond the mean. Using the same methods as applied to unknowns and treating all whole-rock glasses besides KL2G as secondary reference materials, this routine yielded values accurate to <10% for all elements, except (i) Be, Cr, Ni, Co, Ge, and W that were accurate to <20% and (ii) As, Se, Mo, Cd, In, Sn, and Bi that were often >30% inaccurate and hampered by lower concentrations.

2.2. Laser-Induced Breakdown Spectroscopy

Laser-induced breakdown spectroscopy (LIBS) is a type of atomic emission spectroscopy in which a pulsed laser beam of high energy and short duration is focused on a sample to cause material ablation and the generation of a high-temperature microplasma containing its constituent elements. Dissociation and ionization within the plasma led to the generation of a continuum of atomic/ionic emission across UV-visible-near IR wavelengths during plasma cooling. Spectral analysis of this emitted light is used to detect the elements present in the sample.

A SciAps Inc. (Woburn, MA, USA) Z-903 series handheld instrument was used for the LIBS analysis following a similar approach to that described in previous studies [18,19]. This instrument uses a proprietary diode-pumped solid-state 1064 nm Nd-YAG pulsed nanosecond laser that generates a 6 mJ laser pulse with a nominal 100 μm beam size at a 10-Hz firing rate. Pressurized Ar gas is permitted to flow across the sample surface during the time of the analysis for plasma confinement and signal enhancement. The light signal from the plasma emission is typically collected after a 650 ns delay over a 1 ms integration time and passed by fiber optic cable into three spectrometers with time-gated charge-coupled diode detectors that have respective spectral ranges and resolutions as full-width half maximum (FWHM) values of 190 to 365 nm and 0.18 nm, 365 to 620 nm and 0.24 nm,

and 620 to 950 nm and 0.35 nm. This analytical procedure produces a composite broadband LIBS spectrum over more than 23,000 channels of the detector/spectrometer system.

LIBS is capable of quantitative analysis via the development of element-specific calibration curves. For this study, calibration curves were developed for Li, K, and Rb in muscovite on the Z-903 analyzer using its proprietary *Profile Builder* software. Since no suite of certified reference muscovites was available, the calibration curves were generated over the concentration ranges of interest (0 to 0.15 wt. % for Li, 8 to wt. 10% for K, and 0 to 0.6 wt. % for Rb) using a suite of micas previously analyzed for K by EMP analysis and for Li and Rb by LA-ICP-MS analysis. The Z-903 is configured to raster the laser beam across a 2 mm segment of the sample surface and a 4 × 3 point raster grid was used for this study, with three ‘cleaning’ shots and five data acquisition shots made at each point of the grid. These 60 measurements were averaged to produce a single composite spectrum for each location and then five such spectra acquired at different locations on the sample surface were averaged to obtain the Li, K, and Rb abundance estimates from the elemental calibration curves. The mean analytical uncertainty around concentration estimates for the more than 350 muscovites analyzed in this study is 21.8% for Li, 3.3% for K, and 26.1% for Rb.

3. Results and Discussion

3.1. K/Rb and Li Behavior in Pegmatitic Muscovite

The behavior of rare alkali elements in muscovite during the crystallization of pegmatite melts is well documented and, in general, increases with increasing degrees of fractionation [1,8]. As reviewed in Černý et al. [8], Černý and Burt [9], and Hawthorne and Černý [20], the crystal structure of muscovite ideally consists of an Al-O octahedral sheet sandwiched between two (Si,Al)-O tetrahedral sheets to form TOT or 2:1 layers that are bonded together by interlayer K cations. During the crystallization of a pegmatite-forming melt, Rb and Cs may substitute for K in the interlayer site of the muscovite structure whereas Li mainly substitutes for Al in the octahedral sheet. The incorporation of Li, Rb, and Cs into the muscovite structure is a function of their availability in the melt and the presence of competing crystallizing mineral phases. A relatively continuous evolutionary trend of decreasing K/Rb ratios with increasing Li, Rb, and Cs concentrations from the most chemically primitive outermost zones to more evolved interior zones in zoned pegmatites has commonly been observed for Group 1 (LCT) pegmatites e.g., [21–23]. Moreover, decreasing K/Rb with increasing Li, Rb, and Cs trends in muscovite are also exhibited in the sequence of common pegmatites lacking rare-element mineralization through beryl ± columbite ± phosphate-bearing pegmatites to spodumene- and petalite-bearing bodies found in regionally zoned pegmatite populations e.g., [21,24,25].

In this compilation, we note that the Li contents and K/Rb ratios of muscovite from different pegmatite types exhibit a high degree of variability (Tables 1–6). Muscovite from common pegmatites typically exhibits high K/Rb ratios that range mostly from 650 to 40 (Table 1). The Li content of these muscovites is generally low (<200 ppm) but, infrequently, may reach as high as 750 ppm in pegmatites with K/Rb ratios as low as 26 (e.g., Panceiros pegmatite, Spain [26]). Muscovite from (Be-Nb-Ta-P)-enriched pegmatites displays Li concentrations ranging from 20 to 1000 ppm, with the highest values commonly observed in muscovite from pegmatites that contain the Li-phosphates triphylite-lithiophilite or amblygonite-montebbrasite (Table 2). Most K/Rb ratios for muscovite from (Be-Nb-Ta-P)-enriched pegmatites fall between 45 and 10; however, unusually high ranges of 275 to 142 and 141 to 65 were reported in muscovite from the beryl-bearing Henryton pegmatite (Maryland, USA [27]), and from the anatectic pegmatites of the eastern Alps [28], respectively. The Li contents of muscovite from spodumene-bearing pegmatites are among the highest of all the pegmatite types compiled in this study, ranging between 10,000 and 500 ppm (Table 3). Muscovite from spodumene pegmatites display K/Rb ratios as low as 1.4 (e.g., Volta Grande pegmatites, Brazil [29]) to as high as 84 (e.g., Aclare pegmatite, Ireland [30]), although most K/Rb values fall between 40 and 10, a range similar to that for the (Be-

Nb-Ta-P)-enriched pegmatites. The lithium content of muscovite from petalite-bearing pegmatites ranges from 511 to 18,343 ppm, with correspondingly very low K/Rb ratios that range from 10 to 2 (Table 4). As noted by Černý [31], lepidolite subtype pegmatites are not generally widespread compared to other Li-rich rare-element pegmatites and, as such, published analyses of muscovite are not expected to be common. The Li content of muscovite from lepidolite subtype pegmatites available from the literature exhibit a range of values from approximately 20,000 to 800 ppm (Table 5) and their K/Rb ratios range from 55 to 1.5.

Table 1. Partial analyses of muscovite from 63 common pegmatites.

Locality	Li (ppm)	Rb (ppm)	Cs (ppm)	F (%)	K/Rb	References
Ago-Iwoye area, Nigeria (n = 4)	11–16	349–679	15–40	-	617–61	[32]
Cap de Creus field, Spain (n = 9)	14–27	489–598	13–19	0–0.28	178–145	[33]
Cherokee-Pickens district, Georgia, USA (n = 21)	9–121	230–760	-	0.03–0.2	339–106	[34]
Cross Lake field, Manitoba, Canada (n = 38)	14–678	158–2528	9–741	-	508–34	[35]
Diamond Mica mine, South Dakota, USA (n = 3)	445–688	1847–2700	84–139	0.5–1.29	45–30	[36]
Panceiros peg., Spain (n = 5)	232–743	2133–3308	1660–2204	0.21–0.52	39–26	[26]
Rattlesnake mine, South Dakota, USA (n = 3)	159–226	1400–1909	47–51	0.4–0.45	58–42	[36]
Red Sucker Lake field, Manitoba, Canada (n = 5)	47–186	454–1870	15–80	-	188–43	[37]
Thomaston-Barnesville district, Georgia, USA (n = 123)	9–330	5–1476	-	0.0–0.70	350–49	[38]
Yellowknife field, NWT, Canada (n = 19)	47–186	519–2090	0–108	-	153–38	[39]
Number of analyses (n = 230)	9–743	5–3308	0–2204	0–1.29	617–26	

3.2. K/Rb-Li Diagram for Evaluating Li-Mineralization in Granitic Pegmatites

The K/Rb versus Li plot, first utilized by Černý and Burt [9], was extensively used by pegmatite researchers to evaluate the geochemical evolution and degree of fractionation of individual pegmatite bodies and pegmatite groups. This diagram highlights variations in Li content and K/Rb ratios of muscovite from different pegmatite types and illustrates the continuity in fractionation of Li and Rb from muscovite to lithian muscovite to lepidolite in pegmatites of different types. However, meaningful interpretation of the plot is hindered by the limited data available at the time of the Černý and Burt [9] study. The plot does not establish clear boundaries that differentiate between muscovite, lithian muscovite, and lepidolite, common to complex pegmatite types, or pegmatites with different styles of Li-mineralization.

Muscovite is far more common and abundant in Group 1 (LCT) pegmatites than in Group 2 (NYF) pegmatites; nevertheless, during this study, we observed a suitable number of muscovite analyses from Group 2 (NYF) pegmatites to warrant a comparison of muscovite data for the two pegmatite types. Muscovite-bearing Group 2 (NYF) pegmatites with two distinctly different styles of rare-element mineralization were considered in this study: (i) pegmatites that host beryl ± columbite ± REE-minerals such as allanite-(Ce), samarskite-(Y), or gadolinite-(Y) and (ii) pegmatites that are characterized by abundant amazonitic microcline and/or topaz. Lithium mineralization is typically absent or rare at best, occurring primarily as ferroan lepidolite.

Table 2. Partial analyses of muscovite from 53 (Be-Nb-Ta-P)-enriched pegmatites.

Locality	Li (ppm)	Rb (ppm)	Cs (ppm)	F (%)	K/Rb	References
Cap de Creus field (BYL pegs.), Spain (n = 48)	15–285	929–6970	4–2178	0–1.0	89–13	[33]
Cap de Creus field (BCP pegs.), Spain (n = 51)	15–307	1631–8935	9–662	0–0.71	54–10	[40]
Cherokee-Pickens district, Georgia, USA (n = 18)	5–603	420–3107	-	0.07–0.73	196–27	[34]
Cross Lake field, Manitoba, Canada (n = 25)	5–228	1174–4420	31–2660	-	75–19	[35]
Dan Patch peg., South Dakota, USA (n = 6)	311–494	1988–2910	70–127	0.68–0.95	41–29	[36]
Eastern Alps, Italy (n = 7)	86–231	457–9693	-	0.10–0.21	141–8	[28]
El Peñon peg., Argentina (n = 3)	232–418	3018–6584	-	-	28–13	[41]
Henryton peg., Maryland, USA (n = 13)	77–383	323–618	13–37	-	275–142	[27]
Kalu'an field, China (n = 5)	491–1728	1312–2878	76–111	-	53–26	[42]

Table 2. Cont.

Locality	Li (ppm)	Rb (ppm)	Cs (ppm)	F (%)	K/Rb	References
Peerless peg., South Dakota, USA (n = 5)	346–805	1763–2226	53–179	0.87–1.18	45–36	[36]
Yellowknife field (BYL pegs.), NWT, Canada (n = 11)	47–975	1280–7660	16–261	-	63–11	[39]
Yellowknife field (BCP pegs.), NWT, Canada (n = 27)	93–1068	693–9600	12–1140	-	112–7	[39]
Yitt-B peg., Manitoba, Canada (n = 3)	121–149	4206–6035	160–443	-	19–13	[43]
Number of analyses (n = 222)	5–1728	323–9693	4–2660	0–1.18	275–7	

Table 3. Partial analyses of muscovite from 32 spodumene pegmatites.

Locality	Li (ppm)	Rb (ppm)	Cs (ppm)	F (%)	K/Rb	References
Aclare peg., Leinster, Ireland (n = 81)	415–8325	1744–6788	194–2963	0.33–0.80	84–10	[44]
Angwan Doka field, Nigeria (n = 8)	1020–12,500	1245–9400	190–712	0.03–4.5	50–7	[45]
Bailongshan field, China (n = 98)	448–4643	3342–10,717	41–1473	-	26–8	[46]
Cross Lake field, Manitoba, Canada (n = 29)	37–488	1374–32,820	190–2334	-	62–2	[35]
Dumper Dew peg., Maine, USA (n = 41)	584–7078	2853–7910	207–1094	1.89–2.67	82–10	[47]
Harding peg., New Mexico, USA (n = 7)	1115–18,162	5029–12,436	189–4150	-	14–7	[48]
Jiada field, China (n = 11)	1160–3848	3666–7466	181–463	0–0.30	23–11	[49]
Kalu'an field, China (n = 1)	1042	4616	92	-	21	[42]
Moylisha peg., Leinster, Ireland (n = 31)	564–17,158	311–6291	255–990	0.46–5.41	280–14	[30]
Moose II peg, Yellowknife, NWT, Canada (n = 32)	35–1022	2808–8370	44–484	-	32–11	[50]
Peg Claims, Maine, USA (n = 6)	557–1765	1920–3018	-	-	36–24	[51]
Pusila, Tibet (n = 2)	1486–1533	13,442–14,082	566–660	0.03–0.05	6	[52]
Red Sucker Lake field, Manitoba, Canada (n = 4)	7618–9383	19,300–20,300	1660–1950	-	4	[37]
Talati #1 peg., China (n = 20)	627–2599	5930–17,096	223–4143	-	16–5	[53]
Volta Grande, Minas Gerais, Brazil (n = 11)	1208–17,187	689–48,372	754–6414	0.73–0.84	3–1	[29]
Xiaohusite #91 peg., China (n = 10)	652–2170	4503–8289	176–1746	-	20–11	[53]
Number of analyses (n = 392)	35–18,162	311–48,372	41–6414	0–5.41	280–1	

Table 4. Partial analyses of muscovite from seven petalite pegmatites.

Locality	Li (ppm)	Rb (ppm)	Cs (ppm)	F (%)	K/Rb	References
Bikita peg., Zimbabwwe (n = 44)	8243–18,582	19,011–33,541	324–1046	-	5–2	Shaw (pers. comm. 2022)
Buck Claim, Manitoba, Canada (n = 14)	1951–14,771	7224–19,934	283–4056	-	10–4	[54]
Lower Tanco peg., Manitoba, Canada (n = 25)	929–15,607	17,950–30,430	1440–7800	-	4–2	[55]
Presqueira peg., Spain (n = 5)	139–418	3602–4881	1963–4829	0.14–0.33	23–17	[26]
Santa Elena peg., Argentina (n = 4)	1347–16,954	2286–23,043	-	-	39–4	[41]
Tanco peg., Manitoba, Canada (n = 12)	511–17,561	12,253–38,039	1038–7640	0.12–5.25	7–2	[22]
Varutrask peg., Sweden (n = 9)	3205–18,116	3200–13,716	0–7074	0.51–4.60	27–6	[56]
Number of analyses (n = 113)	139–18,582	2286–38,039	0–7800		39–2	

Table 5. Partial analyses of muscovite from eight lepidolite pegmatites.

Locality	Li (ppm)	Rb (ppm)	Cs (ppm)	F (%)	K/Rb	References
Bob Ingersoll peg., South Dakota, USA (n = 13)	929–18,116	3475–10,516	189–1415	0.85–1.74	26–8	[7]
Brown Derby peg., Colorado, USA (n = 5)	3072–14,279	16,601–26,599	849–9715	0.30–6.40	6–4	[57]
Dobrá Voda peg., Czech Republic (n = 1)	1905	6127	189	1.06	14	[58]
Namivo peg., Mozambique (n = 11)	743–17,834	3932–15,454	0–1509	0.50–2.46	21–5	[59]
Reung Kiet mine, Phangnga, Thailand (n = 1)	13,935	9100	2000	3.8	8	[60]
Pidlite peg., New Mexico, USA (n = 1)	4068	8772	1886	0.46	11	[61]
Red Cross Lake field, Manitoba, Canada (n = 5)	2407–16,520	30,466–49,897	3584–12,828	0.37–2.50	3–2	[62]
Rožná peg., Czech Republic (n = 5)	790–1904	1554–6492	94–566	0.64–1.74	55–13	[58]
Number of analyses (n = 42)	743–17,834	236–49,897	0–12,828	0.37–6.4	1.55–2	

Table 6. Partial analyses of muscovite from 60 Group 2 (NYF) pegmatites.

Locality	Li (ppm)	Rb (ppm)	Cs (ppm)	F (%)	K/Rb	References
Falun field, Sweden (n = 7)	64–1371	1258–4756	7–714	-	65–17	[63]
Huron Claim peg., Manitoba, Canada (n = 6)	360–440	10,300–11,400	250–320	0.06–0.12	7–6	[64]
Itabira field, Brazil (n = 40)	19–2069	280–13,330	0–270	0.13–2.2	305–19	[65]
Mangodara district, Burkina Faso (n = 43)	65–578	135–2208	-	-	691–41	[66]
Shatford Lake group, Manitoba, Canada (n = 73)	403–15,690	1006–10,607	377–6886	0.3–5.1	92–8	Buck (unpub. data)
Spro peg., Norway (n = 11)	161–2856	914–2195	0–660	0.2–1.4	90–41	[67]
Tordal and Evje-Iveland fields, Norway (n = 12)	50–12,791	339–20,448	5–12,753	0.89–6.51	284–4	[68]
Number of analyses (n = 192)	19–15,690	315–20,448	0–12,753	0.06–6.51	691–4	

Based on our compilation of previously published muscovite analyses, a modified version of the K/Rb-Li plot presented by Wise et al. [18] was developed that better summarizes the relationship between Li enrichment and the K/Rb fractionation index for different pegmatite types and is better suited for evaluating potential Li-mineralization (Figures 1–5). Boundaries that define distinct levels of fractionation (e.g., poorly fractionated, moderately fractionated, and highly fractionated) were set at K/Rb values of 40 and 10 based on the published muscovite data, overall mineral assemblages, and chemical characteristics of the pegmatites considered in this study.

Moderately fractionated and highly fractionated fields are each divided into two subfields that correspond to chemically distinct types of rare-element mineralization: (i) the (Be-Nb-Ta-P)-enriched but Li-poor pegmatites and (ii) the Li-rich pegmatites. The critical boundary between the Li-poor and Li-rich fields is set at 500 ppm Li, which appears reasonable since the Li concentrations of muscovite from most spodumene-, petalite-, and lepidolite-bearing pegmatites generally exceed that amount.

Most of the published muscovite data from common pegmatites affiliated with Group 1 (LCT) fields have K/Rb ratios > 40 and plot within the field designated as poorly fractionated (Figure 1). This field includes not only pegmatites that are part of rare-element class pegmatite groups and fields (e.g., Black Hills, South Dakota, USA [36]; Red Sucker Lake, Manitoba, Canada [37]; Yellowknife; and Northwest Territories, Canada [39]), but also some pegmatites belonging to the muscovite class (e.g., Thomaston and Cherokee-Pickens fields, Georgia, USA [34,38]). Muscovite data from barren muscovite class pegmatites of the North Baikalian pegmatite belt (data of Manuylov et al. [69] summarized by Černý and Burt [9]) plot well within our expected field of poorly fractionated pegmatites. Similarly, muscovite from mineralogically simple anatectic pegmatites from the Austroalpine area of the Eastern Alps in central Europe reported by Schuster et al. [70] have a primitive geochemical signature and plot primarily in the poorly fractionated field of the K/Rb-Li diagram. The K/Rb ratios and Li values of muscovite from Group 2 (NYF) common pegmatites that lack REE-minerals but that may host accessory garnet, magnetite, or titanite (e.g., Mangodara area, Burkina Faso [66]) also plot within the poorly fractionated portion of the K/Rb-Li diagram (Figure 5).

Muscovite from Group 1 (LCT) pegmatites where beryl or columbite-group minerals are the principal expression of rare-element mineralization can generally be considered as moderately fractionated according to Figure 2. Notable exceptions include the Henryton pegmatite (Maryland, USA [27]); parts of the Peg Group, Yellowknife pegmatite field, (NWT, Canada [39]); and a few localities from the Cherokee-Pickens field (GA, USA [34]), where the muscovite chemistry suggests significantly lower degrees of fractionation.

Moreover, in the Itabira pegmatite area of eastern Brazil, beryl- and columbite-bearing pegmatites considered to be related to anorogenic granites by Marciano [65] fit the Group 2 (NYF) classification of Wise et al. [5] and host muscovite with K/Rb and Li values that plot within the poorly- to moderately-fractionated fields of Figure 5. In general, muscovite from Group 1 (LCT) pegmatites that contain appreciable columbite-group minerals have higher Li concentrations than muscovite from pegmatites with only beryl mineralization. Furthermore, muscovite with elevated Li concentrations from beryl ± columbite Group 1

(LCT) pegmatites may be associated with primary lithium phosphates such as triphylite-lithiophilite or amblygonite-montebrazite whereas this relationship does not appear to be true for Group 2 (NYF) pegmatites.

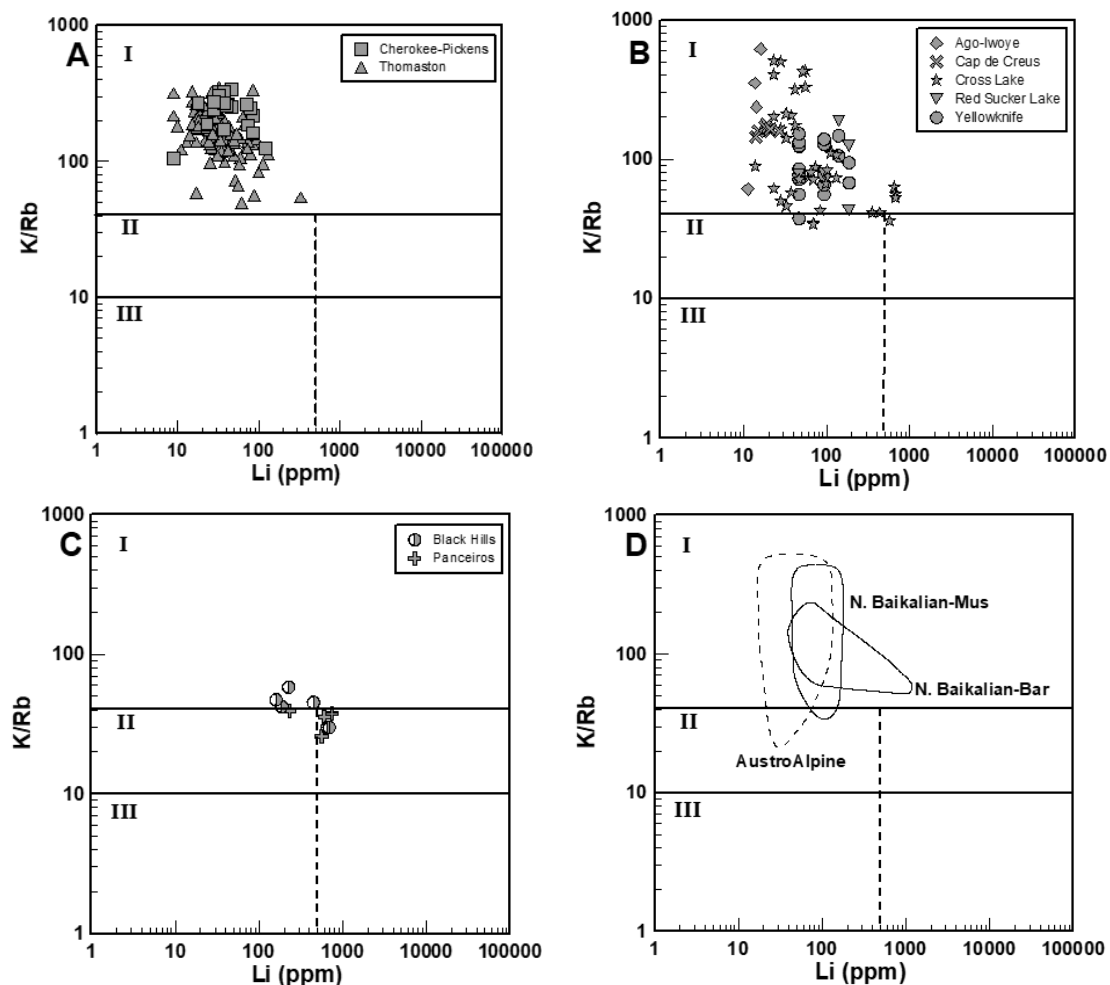


Figure 1. Plot of K/Rb vs Li in muscovite for common pegmatites. Heavy solid lines— boundary between degrees of pegmatite fractionation: I—poorly fractionated, II—moderately fractionated, III—highly fractionated. Short dashed line—boundary between Li-poor and Li-rich pegmatites. Data for (A) muscovite class pegmatite fields; (B) rare-element class pegmatite fields; (C) Black Hills pegmatite field and Panceiros pegmatite; (D) barren (Bar) and muscovite-bearing (Mus) North Baikalia muscovite class pegmatites (after Manuylova et al. [69]) and anatectic AustroAlpine pegmatites (after Knoll et al. [71]).

The K/Rb-Li plots for Group 1 (LCT) pegmatites characterized by substantial Li mineralization show that muscovite may have similar K/Rb ratios but significantly higher Li concentrations compared to (Be-Nb-Ta-P)-enriched pegmatites. The muscovite data of spodumene-bearing pegmatites indicate a moderate degree of fractionation for most of the localities considered in this compilation (Figure 3a,b), whereas muscovite from petalite-bearing pegmatites generally signal higher levels of fractionation (Figure 3c). As seen in Figure 3d, the degree of fractionation for lepidolite-subtype pegmatites are reasonably comparable to those of the spodumene and petalite subtype pegmatites. Conversely, some muscovite data from amazonite- and topaz-bearing Group 2 (NYF) pegmatites plot within the same parts of the K/Rb-Li diagram suggests Li mineralization (e.g., Falun, Sweden [63], Itabira, Brazil [65], and Upper Hoydalen, Norway [68]). However, neither

spodumene nor petalite occur in these pegmatites and only ferroan lepidolite was reported from Hoydalen [68].

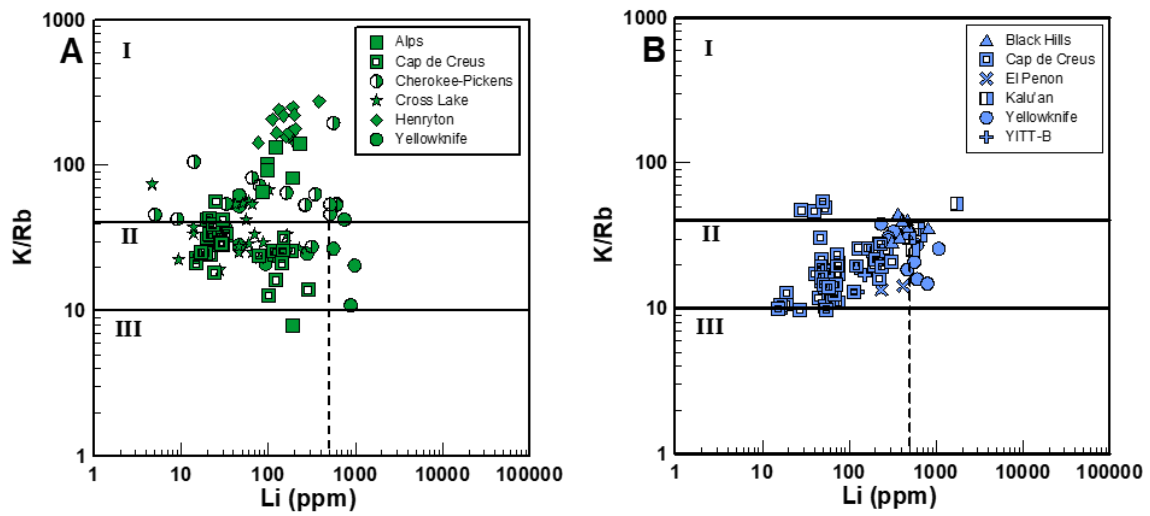


Figure 2. Plot of K/Rb vs Li in muscovite for (A) beryl pegmatites and (B) beryl-columbite-phosphate pegmatites.

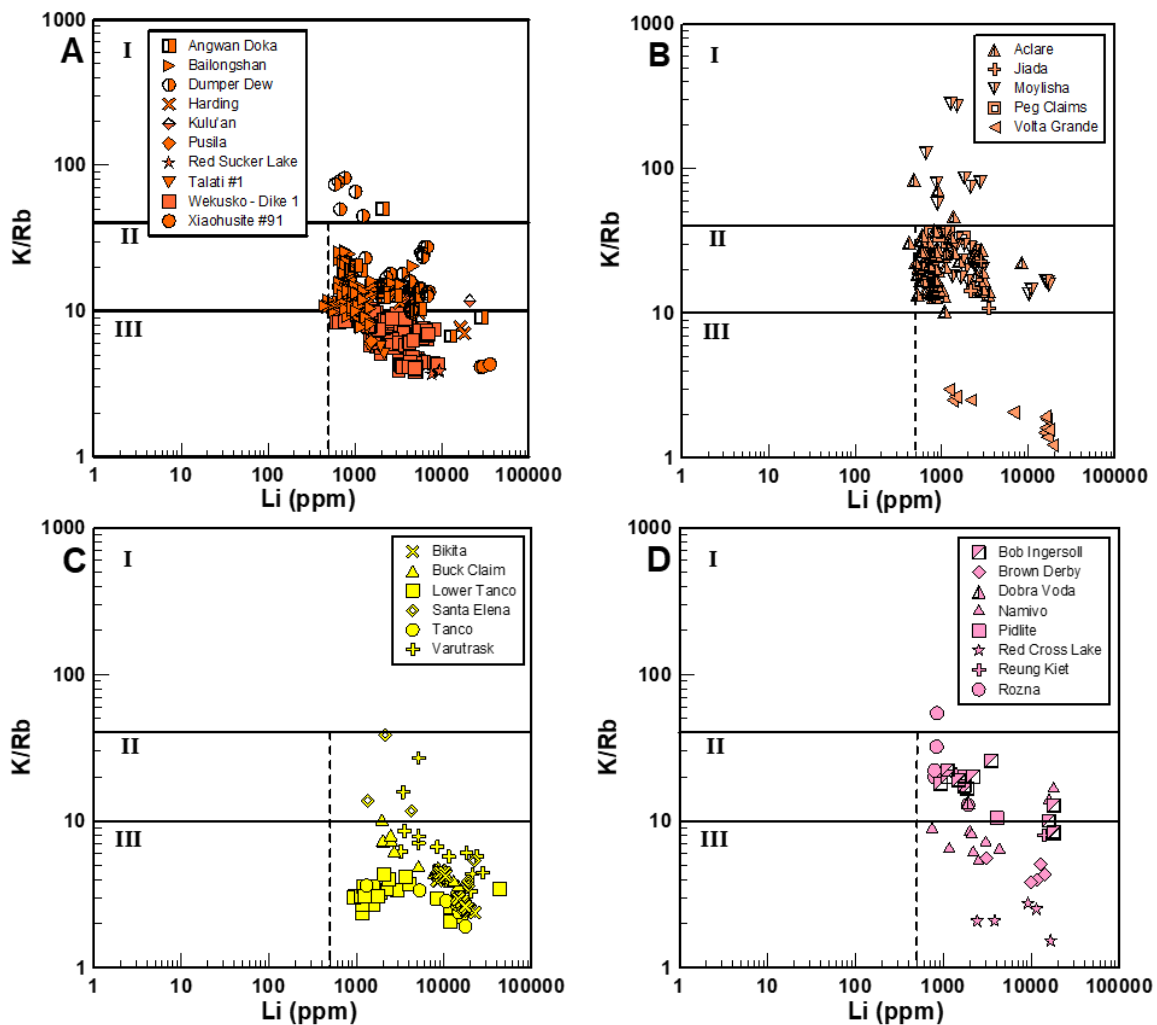


Figure 3. Plot of K/Rb vs Li in muscovite for lithium-rich pegmatites. Data for (A) spodumene pegmatites; (B) spodumene-albite pegmatites; (C) petalite pegmatites; and (D) lepidolite pegmatites.

While the majority of muscovite from Li-rich pegmatites attain Li concentrations ≥ 500 ppm, a few spodumene- and petalite-bearing pegmatites stand out due to their significantly lower Li contents in muscovite (Figure 4a). Muscovite data from the Moose II pegmatite of the Yellowknife field [50] and several spodumene pegmatites from the Cross Lake [35] areas of Canada and the Black Hills, SD, USA [36], fields show considerably lower Li contents ranging from about 20 to 300 ppm. Low Li concentrations of 139 to 418 ppm also characterize the muscovite population from the petalite-bearing Presqueira pegmatite, Spain [26]. Each of these examples plot within the moderately fractionated field generally dominated by (Be-Nb-Ta-P)-enriched pegmatites.

It should be noted that data points of some muscovites from Li-rich pegmatites plot within the field of poorly fractionated pegmatites (Figure 4a). Closer inspection of the data indicates that those analyzed muscovite were sampled from the border and wall zones of pegmatites that are geochemically primitive compared to other zones within the pegmatite. Early crystallizing zones of granitic pegmatites are typically the least fractionated and generally carry minor, if any, amounts of rare-element minerals. Consequently, it is not surprising to observe that muscovite from border and wall zones have higher K/Rb values compared to muscovite from later crystallizing zones. Figure 4a illustrates the variation of Li and K/Rb ratios of muscovite in some distinctly zoned spodumene-bearing pegmatites. High K/Rb ratios between 200 to 45 are observed in muscovite from the border and wall zones (e.g., Etta mine, Black Hills, SD, USA [36], and Yamrang pegmatite, Nepal [40]). The K/Rb ratios of muscovite from the wall zone of the Angwan Doka pegmatite (Nigeria), are noticeably less (from 21 to 19), whereas muscovite from the hanging wall of the Mt. Mica pegmatite (ME, USA), has unexpectedly high K/Rb ratios of 891 to 313. These values are more typical of poorly evolved granites rather than fractionated pegmatites. The K/Rb values of intermediate zone muscovite from three of the pegmatites varies from 140 to 12, whereas muscovite from the core and miarolitic cavities often displays values < 20 . Regardless of their absolute values, the K/Rb ratios of muscovite in these pegmatites exhibit a general decrease from the outer to the inner zones.

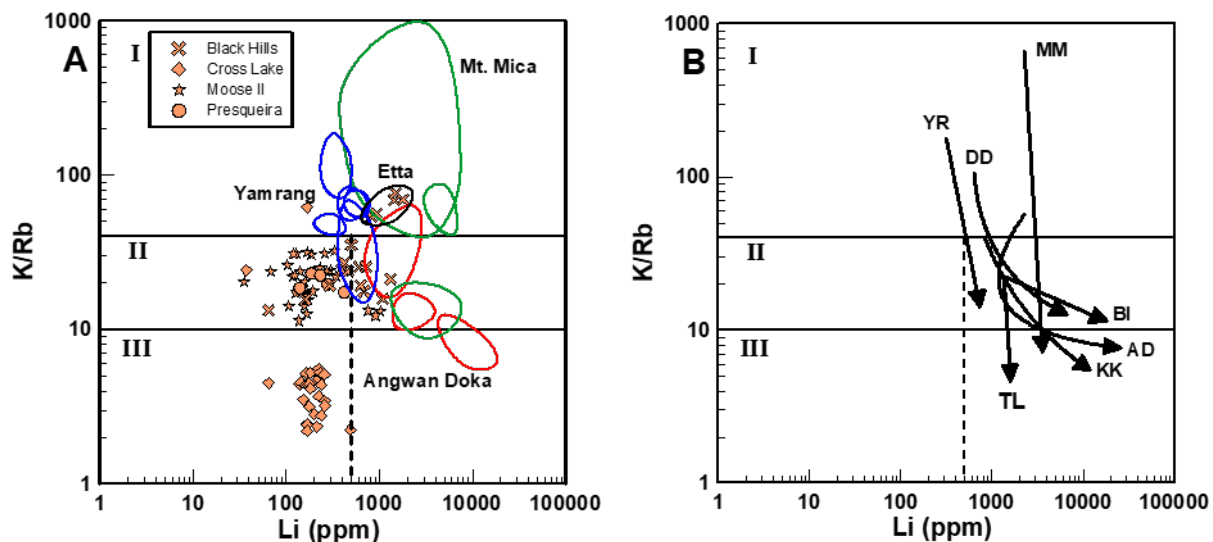


Figure 4. (A) Comparison of K/Rb and Li values for Li-depleted muscovite from spodumene-bearing pegmatites (orange symbols) and Li-enriched muscovite from zoned spodumene pegmatites (colored ellipses). (B) General fractionation trends of muscovite for selected Li-rich pegmatites. Arrows show trends from primitive outer zones (e.g., border and wall) through moderately evolved inner zones (e.g., intermediate) to most evolved interior zones and units (e.g., cores and miarolitic cavities). AD—Angwan Doka, Nigeria; BI—Bob Ingersoll, South Dakota; DD—Dumper Dew, Maine; KK—Koktokay #3, China; MM—Mt. Mica, Maine; TL—Talati No. 1, China; YR—Yamrang, Nepal.

The fractionation paths of muscovite that characterize the internal evolution of spodumene-type pegmatites illustrated in Figure 4b consist of (i) steep trends that feature marked K/Rb fractionation with nearly constant Li content and (ii) limited concurrent trends displaying rapid and extensive K/Rb fractionation prior to pronounced Li enrichment. Presently, the current database is too limited for meaningful explanation of the observed trends and it remains to be determined if similar trends exist for other rare-element pegmatite types.

Comparison of the K/Rb-Li systematics of muscovite from Group 1 (LCT) and Group 2 (NYF) type pegmatites show that pegmatites from the Group 2 category cover similar degrees of fractionation as Group 1 pegmatites (Figures 1–5). The range of K/Rb ratios in muscovite is similar for both major pegmatite associations. Overall, the K/Rb ratios of muscovite from Group 2 (NYF) pegmatites range from 700 to 8 (Table 6), with most of the values falling between 100 to 10, whereas Group 1 (LCT) muscovite have K/Rb values of 600 to 2. With respect to Li enrichment, the Li content of muscovite from Group 1 (LCT) pegmatites varies from nearly 19,000 to 10 ppm, whereas muscovite from Group 2 (NYF) affiliated pegmatites exhibits a slightly narrower range of Li values that varies between 13,000 to 50 ppm.

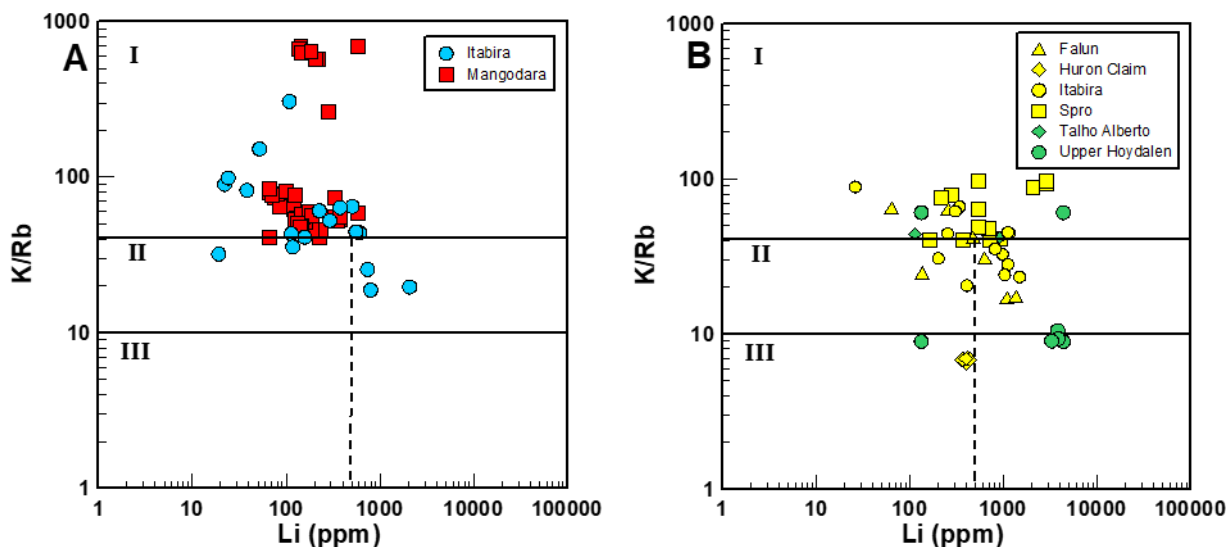


Figure 5. Plot of K/Rb vs Li in muscovite for Group 2 (NYF) pegmatites. Data for (A) common pegmatites (red symbols) and beryl + columbite pegmatites (blue symbols) and (B) topaz-bearing pegmatites (yellow symbols) and amazonite-bearing pegmatites (green symbols).

3.3. Application of K/Rb-Li Diagram as an Exploration Tool

As a test of the functionality of the K/Rb versus Li diagram, we plotted our own muscovite data of 180 analyses determined by LA-ICP-MS (Figure 6a) and LIBS (Figure 6b–d). Our samples of coarse-grained platy primary muscovites were extracted from pegmatites of the muscovite class, beryl-columbite-phosphate, spodumene, petalite, and spodumene-albite pegmatites of Group 1 (LCT) affiliation. The samples represent pegmatites from the Oxford pegmatite field (Maine, USA); the Spruce Pine pegmatite district (North Carolina, USA); and several localities visited by W.E. Heinrich during his extensive investigation of the mica group from 1942 to about 1955. Figure 6a shows that the K/Rb-Li systematics of muscovite accurately reflects the degree of fractionation achieved by our sampled pegmatites and, in most cases, correctly predicts the type of rare-element mineralization expected in each pegmatite. The K/Rb values of muscovite from beryl-bearing pegmatites may seem higher than expected but this could be a result of sampling from primitive zones of the pegmatites. In the case of the Tourmaline Queen pegmatite (CA, USA), Li mineral-

ization is represented by an abundance of elbaite and lepidolite rather than spodumene or petalite and the K/Rb ratios and Li contents of muscovite clearly reflect this observation.

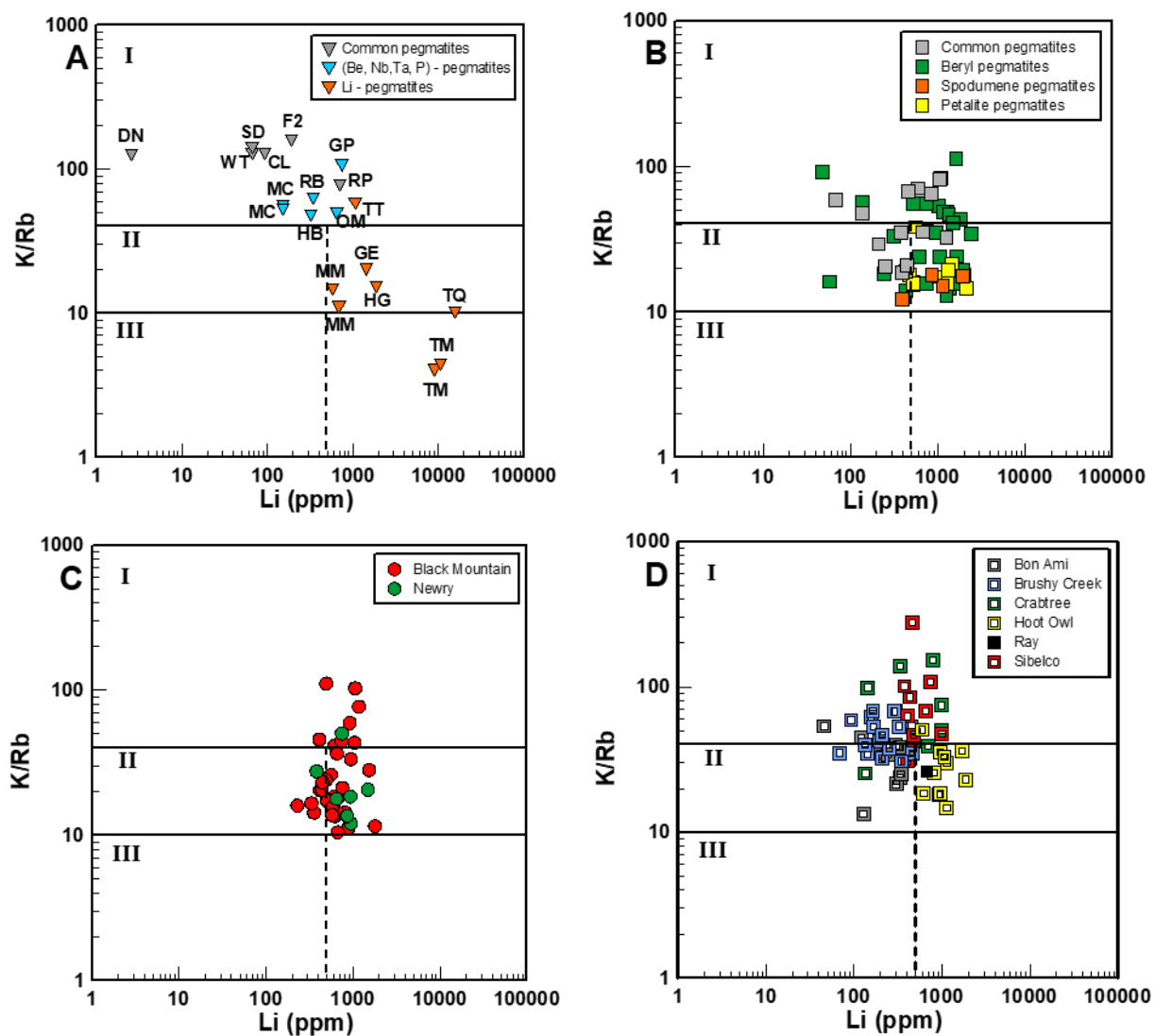


Figure 6. Plots of K/Rb versus Li for muscovite analyzed by LA-ICP-MS (A) and handheld LIBS (B–D). (A) Miscellaneous pegmatite localities: CL—Collum, Alabama; DN—Doc Nicols, North Carolina; F2—Friendship #2, Alabama; GE—General Electric #3—Maine; GP—Gap Lode. South Dakota; HB—Hibbs, Maine; HG—Hugo, South Dakota; MC—Muscovite Claim, Idaho; MM—Mt. Mica, Maine; OM—Old Mike, South Dakota; RB—Riber, NWT, Canada; RP—Rudasill prospect, North Carolina; SD—Silver Dollar, South Dakota; TM—Tin Mountain, South Dakota; TQ—Tourmaline Queen, California; TT—Twin Tunnels, Maine; WT—W.T. Foster, North Carolina. (B) Sebago pegmatite group, Maine; (C) Spodumene pegmatites of the Rumford pegmatite group, Maine; (D) Common pegmatites (Bon Ami, Hoot Owl, Sibelco), beryl pegmatites (Brushy Creek, Crabtree) and spodumene pegmatite (Ray) of the Spruce Pine pegmatite district, North Carolina.

Laser-induced breakdown spectroscopy (LIBS) is an analytical technique that is becoming increasingly popular as a tool for critical mineral exploration [72–74]. The recent development of handheld LIBS instruments permits the rapid acquisition of compositional data on-site in the field, thus making it an attractive tool for granitic pegmatite mineral exploration. With careful calibration, the LIBS instrument can quantitatively measure Li concentrations and calculate K/Rb ratios in muscovite, which can then be used for evaluation of the level of pegmatite fractionation and the style of rare-element mineralization.

Wise et al. [18] and Harmon et al. [19] demonstrated the ability of a handheld LIBS instrument to effectively examine the potential for Li enrichment in barren and fertile, i.e., mineralized) pegmatites from the Carolina Tin-Spodumene Belt (CTSB) of western North Carolina, USA. Quantitative LIBS analysis of muscovite across the CTSB by Harmon et al. [19] revealed that, in general, high Li contents and low K/Rb ratios were typical of spodumene-bearing pegmatites relative to non-spodumene-bearing pegmatites. They concluded that LIBS could be a valuable tool for rapid in-field and on-site geochemical analysis of muscovite in support of exploration programs aimed at identifying Li-enriched pegmatites.

Figure 6b–d show the K/Rb ratios and Li content of muscovite as determined by handheld LIBS for a variety of pegmatite types from Maine and North Carolina. In general, our results of the muscovite LIBS analysis favorably reflect the degree of evolution according to the rare-element mineralization observed in the pegmatites. As expected, muscovite from all spodumene- and petalite-bearing pegmatites correctly plots in the moderately fractionated field and are consistent with muscovite K/Rb-Li systematics from spodumene-bearing pegmatites from other worldwide localities. LIBS muscovite data from beryl, beryl-columbite, and beryl-columbite-phosphate subtype pegmatites may straddle or exceed the boundary that differentiates moderately fractionated Li-poor from Li-rich pegmatites.

The distribution, classification, and geological setting of the Oxford pegmatite field of southwestern Maine was described by Wise and Francis [75] and is populated by mineralogically and chemically primitive to complexly zoned and highly fractionated pegmatites that are generally characterized by a Group 1 (LCT)-type mineralogical–geochemical signature [75,76]. The pegmatites vary in character from quasi-homogeneous simple pegmatites through beryl ± columbite ± phosphate-bearing to complex Li-enriched spodumene- and petalite-bearing pegmatites. Pegmatites displaying Group 2 (NYF) characteristics are apparently uncommon. Pegmatites from the Sebago group, located in the southern portion of the Oxford field, and the unrelated Rumford group, situated in the northern part of the field, were the focus of the LIBS muscovite study.

Figure 6b shows that the K/Rb and Li data of muscovite from spodumene-, petalite- and some of the beryl-bearing pegmatites of the Sebago group, corroborate the observed style of rare-element mineralization as reported by Wise and Brown [76]. Muscovite from the spodumene- and petalite-bearing pegmatites of the Sebago group generally exceed the Li concentration of 500 ppm set as the proposed threshold indicating Li-mineralization. Conversely, many of the muscovite samples with Li contents >500 ppm Li collected from beryl-bearing pegmatites do not carry spodumene or petalite; instead, elbaite occurs as the main Li mineral. Additionally, muscovite from some of the common pegmatites of the Sebago group may also exhibit K/Rb and Li ratios that suggest the presence of rare-element mineralization. As of this writing, we cannot confirm the existence of Be- or Li- minerals in these presumably common pegmatites.

Within the Rumford group of the Oxford field pegmatites, the muscovite data of the spodumene-bearing Black Mountain and Newry pegmatites plot within the expected Li-enriched portion of the K/Rb-Li plot (Figure 6c). The few Black Mountain analyses that plot within the poorly fractionated field represent muscovite sampled from the wall zone of the pegmatite.

The pegmatite population of the Spruce Pine area of western North Carolina, USA, is dominated by mineralogically simple pegmatites with few bodies that exhibit noticeable rare-element mineralization. Apart from two pegmatites, which contain rare spodumene or pollucite, the rare-element geochemical signature of the Spruce Pine pegmatite district is best characterized as Be- and Nb-enriched but Li- and Cs-poor. Modest amounts of rare-earth minerals may also occur in some pegmatites such as allanite, euxenite, and samarskite. According to the classification criteria of [6], the Spruce Pine pegmatites can be classified as belonging to the muscovite class.

The LIBS analysis of Spruce Pine muscovite generally confirms the primitive to moderately fractionated nature of the pegmatites within the district. According to Figure 6d, muscovite from most of the Spruce Pine pegmatites examined in this study plot within the expected fields of fractionation and mineralization.

It is notable that the LIBS muscovite data for the Hoot Owl mine clearly suggest the presence of Li minerals. The Hoot Owl pegmatite was extensively mined from 1937 through World War II and intermittently up to 1962 and throughout its mining history, no Li minerals were ever observed or reported. Thus, it is uncertain why the muscovite data plot within the field suggest Li-mineralization. Similarly, muscovite data for the Ray pegmatite also plot within the moderately fractionated Li-enriched field even though its rare-element mineralization is defined by the extremely limited presence of minor elbaite and pollucite, neither of which occurs in economic quantities.

4. Conclusions

The identification of pegmatites that potentially contain significant Li mineralization can be achieved from the study of regional distribution patterns of pegmatite populations in conjunction with quantitative analysis of major and accessory minerals that concentrate Li in minor to trace quantities. Muscovite has been shown to be an important reservoir of Li in moderately- to highly-fractionated pegmatites and the K/Rb-Li systematics of muscovite can provide informative insight into the evolutionary behavior of rare alkali element enrichment with progressive fractionation in granitic pegmatites. While it is generally accepted that the K/Rb fractionation index of primary muscovite serves as a useful indicator for distinguishing primitive from geochemically evolved pegmatites, the overlap of muscovite K/Rb ratios for Group 1 (LCT) and Group 2 (NYF) pegmatites as well as the misclassification of some pegmatite localities shown in this study underscores the challenge of deciphering the significance of the K/Rb-Li systematics as it relates to Li mineralization in a pegmatite. While we have attempted to limit our dataset to include only chemical data acquired from primary muscovite, inadvertent inclusion of secondary muscovite (e.g., muscovite formed by greisenization) could potentially introduce some small uncertainties in our final interpretations which may explain some of the irregularities in the classification of fractionation levels for some localities (e.g., Cross Lake and Presqueira pegmatites). Despite these shortcomings, the following conclusions can be drawn:

1. Muscovite with Li-concentrations in excess of 500 ppm in conjunction with K/Rb ratios < 40 are strong indicators of potential Li mineralization for Group 1 (LCT) pegmatite. However, these parameters are only relevant to pegmatites that can be classified as such with reasonable confidence by the investigator and the application of these same parameters to Group 2 (NYF) pegmatites may lead to erroneous interpretations regarding rare-element mineralization;
2. The positive relationship of elevated Li concentration in muscovite and Li mineralization in pegmatite is best exhibited in pegmatites of Group 1 (LCT) affiliation. However, for Group 2 (NYF) pegmatites, the gradual increase in Li content of muscovite over the sequence: common quartz-feldspar to beryl \pm columbite \pm REE-minerals to amazonite- or topaz-bearing pegmatites, does not equate to a concomitant increase in the crystallization of Li minerals with advancing pegmatite fractionation;
3. Muscovite displaying high K/Rb ratios with high Li values may not always imply crystallization of a poorly fractionated pegmatite with unfavorable rare-element mineralization. Geochemically primitive pegmatite zones and assemblages that develop during the early stages of Li-rich pegmatite crystallization can host muscovite with high fractionation indexes.

To ensure a fairly accurate evaluation of the potential Li mineralization from an individual pegmatite body or a pegmatite population, we recommend the collection and analysis of a sufficient number of primary muscovite samples, preferably extracted from several different pegmatite zones but ideally from the most fractionated part of the pegmatite where possible. A minimum of three to five unweathered/unaltered coarse-grained

platy muscovite specimens should be acquired from the most interior zones or units of the pegmatite that represent primary crystallization (e.g., inner intermediate zones adjacent to quartz cores or blocky K-feldspar + quartz + muscovite assemblages in the central parts of the pegmatite if distinct quartz cores are not developed) is most desirable. For pegmatite exploration programs requiring the analysis of multiple samples from several pegmatite bodies, a field-based instrument, such as a handheld LIBS analyzer, may prove indispensable in expediting the acquisition of quantitative K/Rb and Li values from numerous samples in support of evaluating rare element mineralization potential.

Author Contributions: M.A.W. defined and led the study. M.A.W. undertook the fieldwork in ME and all authors participated in the NC fieldwork. A.C.C. undertook the EPMA and LA-ICP-MS analyses. R.S.H. developed the K, Rb, and Li calibrations for the Z-903 LIBS instrument and conducted the LIBS analyses. M.A.W. prepared the paper with review from all co-authors. All authors have read and agreed to the published version of the manuscript.

Funding: Funding for the LIBS analyzer was provided by North Carolina Policy Collaboratory grant #207586-50004 to North Carolina State University.

Data Availability Statement: The underlying analytical data are still being used for research and, therefore, proprietary. These data will be publicly archived at the completion of our research program.

Acknowledgments: The authors gratefully acknowledge the comments from three anonymous reviewers and the academic editors for their constructive reviews of the manuscript. Our appreciation is extended to Sibelco, specifically Dave DePlato and Aiden King, for logistical support and facilitating the fieldwork at their Spruce Pine North Carolina site. We also thank Alan Schabillion and Kay Buchanan for granting access to various pegmatite mines in the Spruce Pine area. Thanks are extended to Richard Shaw for allowing the use of his unpublished muscovite data from the Bikita pegmatite, Zimbabwe, as well as to Joshua Garber at the LionChron facility at Penn State for his aid in acquiring LA-ICP-MS data and to Lowell Moore at the Electron Microprobe Laboratory in the Department of Geosciences at Virginia Tech for his assistance with the microprobe analysis. We thank the National Museum of Natural History, Smithsonian Institution, and the Peabody Museum of Yale University for providing the reference micas used for the development of the mica calibrations on the LIBS handheld analyzer.

Conflicts of Interest: The authors declare no conflicts of interest.

References

1. Trueman, D.L.; Černý, P. Exploration for Rare-Element Pegmatites. In *Granitic Pegmatites in Science and Industry, Short Course Handbook*; Černý, P., Ed.; Mineralogical Association of Canada: Winnipeg, MB, Canada, 1982; Volume 8, pp. 463–493.
2. Selway, J.B.; Breaks, F.W.; Tindle, A.G. A review of rare-element (Li-Cs-Ta) pegmatite exploration techniques for the Superior Province, Canada, and large worldwide tantalum deposits. *Explor. Min. Geol.* **2005**, *14*, 1–30. [[CrossRef](#)]
3. Beurlen, H.; Thomas, R.; da Silva, M.R.R.; Müller, A.; Rhede, D.; Soares, D.R. Perspectives for Li- and Ta-mineralization in the Borborema Pegmatite Province, NE-Brazil: A review. *J. South Am. Earth Sci.* **2014**, *56*, 110–127. [[CrossRef](#)]
4. Maneta, V.; Baker, D.R. The potential of lithium in alkali feldspars, quartz, and muscovite as a geochemical indicator in the exploration for lithium-rich granitic pegmatites: A case study from the spodumene-rich Moblan pegmatite, Quebec, Canada. *J. Geochem. Explor.* **2019**, *205*, 106336. [[CrossRef](#)]
5. Wise, M.A.; Müller, A.; Simmons, W.B. A proposed new mineralogical classification system for granitic pegmatites. *Can. Mineral.* **2022**, *60*, 229–248. [[CrossRef](#)]
6. Černý, P.; Ercit, T.S. The classification of granitic pegmatites revisited. *Can. Mineral.* **2005**, *43*, 2005–2026. [[CrossRef](#)]
7. Jolliff, B.; Papike, J.; Shearer, C. Fractionation trends in mica and tourmaline as indicators of pegmatite internal evolution: Bob Ingersoll pegmatite, Black Hills, South Dakota. *Geochim. Cosmochim. Acta* **1987**, *51*, 519–534. [[CrossRef](#)]
8. Černý, P.; Meintzer, R.E.; Anderson, A.J. Extreme fractionation in rare-element granitic pegmatites: Selected examples of data and mechanisms. *Can. Mineral.* **1985**, *23*, 381–421.
9. Černý, P.; Burt, D. Paragenesis, Crystallochemical Characteristics, and Geochemical Evolution in Micas in Granite Pegmatites. In *Micas, Reviews in Mineralogy*; Bailey, S.W., Ed.; Mineralogical Society of America: Chantilly, VA, USA, 1984; Volume 13, pp. 257–297.
10. Gordiyenko, V.V. *Mineralogy, Geochemistry and Genesis of the Spodumene Pegmatites*; Nedra, Leningrad: Saint Petersburg, Russia, 1975; 237p.
11. Gordiyenko, V.V. Concentrations of Li, Rb, and Cs in potash feldspar and muscovite as criteria for assessing the rare-metal mineralization in granite pegmatites. *Int. Geol. Rev.* **1971**, *13*, 134–142. [[CrossRef](#)]

12. Smeds, S.-A. Trace elements in potassium-feldspar and muscovite as a guide in the prospecting for lithium- and tin-bearing pegmatites in Sweden. *J. Geochem. Explor.* **1992**, *42*, 351–369. [[CrossRef](#)]
13. Novák, M.; Povondra, P. Elbaite pegmatites in the Moldanubicum: A new subtype of the rare-element class. *Mineral. Petrol.* **1995**, *55*, 159–176. [[CrossRef](#)]
14. Černý, P. Rare-element granitic pegmatites. Part I: Anatomy and internal evolution of pegmatite deposits. *Geosci. Can.* **1991**, *18*, 49–67.
15. Pearce, N.J.; Perkins, W.T.; Westgate, J.A.; Gorton, M.P.; Jackson, S.E.; Neal, C.R.; Chenery, S.P. A compilation of new and published major and trace element data for NIST SRM 610 and NIST SRM 612 glass reference materials. *Geostand. Newsl.* **1997**, *21*, 115–144. [[CrossRef](#)]
16. Jochum, K.P.; Stoll, B.; Herwig, K.; Willbold, M.; Hofmann, A.W.; Amini, M.; Aarburg, S.; Abouchami, W.; Hellebrand, E.; Mocek, B.; et al. MPI-DING reference glasses for in situ microanalysis: New reference values for element concentrations and isotope ratios. *Geochem. Geophys. Geosyst.* **2006**, *7*. [[CrossRef](#)]
17. Paton, C.; Hellstrom, J.; Paul, B.; Woodhead, J.; Hergt, J. Iolite: Freeware for the visualisation and processing of mass spectrometric data. *J. Anal. At. Spectrom.* **2011**, *26*, 2508–2518. [[CrossRef](#)]
18. Wise, M.A.; Harmon, R.S.; Curry, A.; Jennings, M.; Grimac, Z.; Khashchevskaya, D. Handheld LIBS for Li exploration: An example from the Carolina Tin-Spodumene Belt, USA. *Minerals* **2022**, *12*, 77. [[CrossRef](#)]
19. Harmon, R.S.; Wise, M.A.; Curry, A.C.; Mistle, J.S.; Mason, M.S.; Grimac, Z. Rapid analysis of muscovites on a lithium pegmatite prospect by handheld LIBS. *Minerals* **2023**, *13*, 697. [[CrossRef](#)]
20. Hawthorne, F.C.; Černý, P. The Mica Group. In *Granitic Pegmatites in Science and Industry; Mineralogical Association of Canada Short Course Handbook*; Mineralogical Association of Canada: Toronto, ON, Canada, 1982; Volume 8, pp. 63–98.
21. Roda, E.; Keller, P.; Pesquera, A.; Fontan, F. Micas of the muscovite–lepidolite series from Karibib pegmatites, Namibia. *Mineral. Mag.* **2007**, *71*, 41–62. [[CrossRef](#)]
22. Van Lichtervelde, M.; Grégoire, M.; Linnen, R.L.; Béziat, D.; Salvi, S. Trace element geochemistry by laser ablation ICP-MS of micas associated with Ta mineralization in the Tanco pegmatite, Manitoba, Canada. *Contrib. Mineral. Petrol.* **2008**, *155*, 791–806. [[CrossRef](#)]
23. Cao, C.; Shen, P.; Bai, Y.; Luo, Y.; Feng, H.; Li, C.; Pan, H. Chemical evolution of micas and Nb-Ta oxides from the Koktokay pegmatites, Altay, NW China: Insights into rare-metal mineralization and genetic relationships. *Ore Geol. Rev.* **2022**, *146*, 104933. [[CrossRef](#)]
24. Vieira, R.; Roda-Robles, E.; Pesquera, A.; Lima, A. Chemical variation and significance of micas from the Fregeneda-Almendra pegmatitic field (Central-Iberian Zone, Spain and Portugal). *Am. Mineral.* **2011**, *96*, 637–645. [[CrossRef](#)]
25. Li, P.; Li, J.; Chen, Z.; Liu, X.; Huang, Z.; Zhou, F. Compositional evolution of the muscovite of Renli pegmatite-type rare-metal deposit, northeast Hunan, China: Implications for its petrogenesis and mineralization potential. *Ore Geol. Rev.* **2021**, *138*, 104380. [[CrossRef](#)]
26. Roza Llera, A.; Fuertes-Fuente, M.; Cepedal, A.; Martin-Izard, A. Barren and Li–Sn–Ta Mineralized pegmatites from NW Spain (Central Galicia): A comparative study of their mineralogy, geochemistry, and wallrock metasomatism. *Minerals* **2019**, *9*, 739. [[CrossRef](#)]
27. Kearns, C.A. The Mineralogy and Mineral Chemistry of the Henryton Pegmatite, Patapsco State Park, Carroll County, Maryland. Ph.D. Thesis, George Mason University, Fairfax, VA, USA, 2018.
28. Konzett, J.; Schneider, T.; Nedyalkova, L.; Hauzenberger, C.; Melcher, F.; Gerdes, A.; Whitehouse, M. Anatectic granitic pegmatites from the Eastern Alps: A case of variable rare-metal enrichment during high-grade regional metamorphism—I: Mineral assemblages, geochemical characteristics, and emplacement ages. *Can. Mineral.* **2018**, *56*, 555–602. [[CrossRef](#)]
29. Lagache, M.; Quéméneur, J. The Volta Grande pegmatites, Minas Gerais, Brazil: An example of rare-element granitic pegmatites exceptionally enriched in lithium and rubidium. *Can. Mineral.* **1997**, *35*, 153–165.
30. Barros, R.; Kaeter, D.; Menuge, J.F.; Škoda, R. Controls on chemical evolution and rare element enrichment in crystallising albite-spodumene pegmatite and wallrocks: Constraints from mineral chemistry. *Lithos* **2020**, *352*, 105289. [[CrossRef](#)]
31. Černý, P. Characteristics of Pegmatite Deposits of Tantalum. In *Lanthanides, Tantalum and Niobium: Mineralogy, Geochemistry, Characteristics of Primary Ore Deposits, Prospecting, Processing and Applications Proceedings of a workshop in Berlin, November 1986*; Springer: Berlin/Heidelberg, Germany, 1989; pp. 195–239.
32. Akintola, A.I.; Ikhane, P.R.; Okunlola, O.A.; Akintola, G.O.; Oyebolu, O.O. Compositional features of Precambrian pegmatites of Ago-Iwoye area South Western, Nigeria. *J. Ecol. Nat. Environ.* **2012**, *4*, 71–87. [[CrossRef](#)]
33. Serrano, J. Origine des pegmatites du Cap de Creus: Approche intégrée de terrain, pétrologie et géochimie. Ph.D. Thesis, Université Paul Sabatier—Toulouse III, Toulouse, France, 2019.
34. Gunow, A.J.; Bonn, G.N. The geochemistry and origin of pegmatites Cherokee-Pickens district. *Ga. Geol. Surv. Bull.* **1989**, *103*, 93.
35. Anderson, A. The Chemistry, Mineralogy and Petrology of the Cross Lake Pegmatite Field, Central Manitoba. Master’s Thesis, University of Manitoba, Winnipeg, MB, Canada, 1984.
36. Jolliff, B.B.; Papike, J.J.; Shearer, C.K. Petrogenetic relationships between pegmatite and granite based on geochemistry of muscovite in pegmatite wall zones, Black Hills, South Dakota, USA. *Geochim. Cosmochim.* **1992**, *56*, 1915–1939. [[CrossRef](#)]

37. Chackowsky, L.E. Mineralogy, Geochemistry and Petrology of Pegmatitic Granites and Pegmatites at Red Sucker Lake, Northeastern Manitoba. Master's Thesis, University of Manitoba, Winnipeg, MB, Canada, 1987.
38. Cocker, M.D. Geochemistry and Economic Potential of Pegmatites in the Thomaston-Barnesville District, Georgia. In *Geologic Report 7*; Georgia Department of Natural Resources, Environmental Protection Division, Georgia Geologic Survey: Marietta, GA, USA, 1992; 81p.
39. Meintzer, R.E. The Mineralogy and Geochemistry of the Granitoid Rocks and Related Pegmatites of the Yellowknife Pegmatite Field, Northwest Territories. Ph.D. Thesis, University of Manitoba, Winnipeg, MB, Canada, 1987.
40. Bhandari, S.; Qin, K.; Zhou, Q.; Evans, N.J. Geological, mineralogical and geochemical study of the aquamarine-bearing Yamrang pegmatite, Eastern Nepal with implications for exploration targeting. *Minerals* **2022**, *12*, 564. [[CrossRef](#)]
41. Galliski, M.A.; Saavedra, J.; Márquez-Zavalía, M.F. Mineralogía y geoquímica de las micas en las pegmatitas Santa Elena y El Penon, Provincia Pegmatítica Pampeana, Argentina. *Rev. Geol. Chile* **1999**, *26*, 125–137. [[CrossRef](#)]
42. Cen, J.B.; Feng, Y.G.; Liang, T.; Gao, J.G.; He, L.; Zhou, Y. Implications of muscovite composition on the genesis of Li-rich and Be-rich pegmatites: A case study of the Kalu'an rare-metal pegmatite ore-field. *Acta Petrol. Sin.* **2022**, *38*, 411–427.
43. Anderson, S.D.; Černý, P.; Halden, N.M.; Chapman, R.; Uher, P. The Yitt-B pegmatite swarm at Bernic Lake, southeastern Manitoba: A geochemical and paragenetic anomaly. *Can. Mineral.* **1998**, *36*, 283–301.
44. Kaeter, D.; Barros, R.; Menuge, J.F.; Chew, D.M. The magmatic–hydrothermal transition in rare-element pegmatites from southeast Ireland: LA-ICP-MS chemical mapping of muscovite and columbite–tantalite. *Geochim. Et Cosmochim. Acta* **2018**, *240*, 98–130. [[CrossRef](#)]
45. Akoh, J.U.; Ogunleye, P.O. Mineralogical and geochemical evolution of muscovite in the pegmatite group of the Angwan Doka area, Kokoona district: A clue to petrogenesis and tourmaline mineralization potential. *J. Geochem. Explor.* **2014**, *146*, 89–104. [[CrossRef](#)]
46. Xing, C.M.; Wang, C.Y.; Wang, H. Magmatic-hydrothermal processes recorded by muscovite and columbite-group minerals from the Bailongshan rare-element pegmatites in the West Kunlun-Karakorum orogenic belt, NW China. *Lithos* **2020**, *364*, 105507. [[CrossRef](#)]
47. South, J.K. Mineralogy and Geochemistry of the Dumper Dew Pegmatite, Oxford County, Maine. Master's Thesis, University of New Orleans, New Orleans, LA, USA, 2009.
48. Jahns, R.H.; Ewing, R.C. The Harding Mine, Taos County, New Mexico. In *New Mexico Geological Society Guidebook, 27th Field Conference*; New Mexico Geological Society: Socorro, NM, USA, 1976; pp. 263–276.
49. Li, X.; Dai, H.; Wang, D.; Liu, S.; Wang, G.; Wang, C.; Huang, F.; Zhu, H. Geochronological and geochemical constraints on magmatic evolution and mineralization of the northeast Ke'eryin pluton and the newly discovered Jiada pegmatite-type lithium deposit, Western China. *Ore Geol. Rev.* **2022**, 105164. [[CrossRef](#)]
50. Anderson, M.O.; Lentz, D.R.; McFarlane, C.R.; Falck, H. A geological, geochemical and textural study of an LCT pegmatite: Implications for the magmatic versus metasomatic origin of Nb-Ta mineralization in the Moose II pegmatite, Northwest Territories, Canada. *J. Geosci.* **2013**, *58*, 299–320. [[CrossRef](#)]
51. Sundelius, H.W. The Peg claims spodumene pegmatites, Maine. *Econ. Geol.* **1963**, *58*, 84–106. [[CrossRef](#)]
52. Liu, C.; Wang, R.C.; Wu, F.Y.; Xie, L.; Liu, X.C.; Li, X.K.; Yang, L.; Li, X.J. Spodumene pegmatites from the Pusila pluton in the higher Himalaya, South Tibet: Lithium mineralization in a highly fractionated leucogranite batholith. *Lithos* **2020**, *358*, 105421. [[CrossRef](#)]
53. Chen, J.Z.; Zhang, H.; Tang, Y.; Lv, Z.H.; An, Y.; Wang, M.T.; Liu, K.; Xu, Y.S. Lithium mineralization during evolution of a magmatic–hydrothermal system: Mineralogical evidence from Li-mineralized pegmatites in Altai, NW China. *Ore Geol. Rev.* **2022**, 105058. [[CrossRef](#)]
54. Lenton, P.G. Mineralogy and Petrology of the Buck Claim Lithium Pegmatite, Bernic Lake, Southeastern, Manitoba. Master's Thesis, University of Manitoba, Winnipeg, MB, Canada, 1979.
55. Ferreira, K.J. The Mineralogy and Geochemistry of the Lower Tanco Pegmatite, Bernic Lake, Manitoba, Canada. Master's Thesis, University of Manitoba, Winnipeg, MB, Canada, 1984.
56. Quensel, P. The paragenesis of the Varuträsk pegmatite including a review of its mineral assemblage. *Ark. Min. Geol.* **1957**, *2*, 9–126.
57. Elder, R.A. Geochemistry and Mineralogy of the Brown Derby No. 1 Pegmatite, Gunnison County, Colorado. Master's Thesis, University of New Orleans, New Orleans, LA, USA, 1998.
58. Černý, P.; Chapman, R.; Staně, J.; Nová, M.; Baadsgaard, H.; Rieder, M.; Kavalová, M.; Ottolini, L. Geochemical and structural evolution of micas in the Rožná and Dobrá Voda pegmatites, Czech Republic. *Mineral. Petrol.* **1995**, *55*, 177–201. [[CrossRef](#)]
59. Neiva, A.M. Micas, feldspars and columbite–tantalite minerals from the zoned granitic lepidolite-subtype pegmatite at Namivo, Alto Ligonha, Mozambique. *Eur. J. Mineral.* **2013**, *25*, 967–985. [[CrossRef](#)]
60. Garson, M.S.; Bradshaw, N.; Rattawong, S. Lepidolite Pegmatites in the Phangnga Area of Peninsular Thailand. In *2nd Technical Conference on Tin 1*; Fox, W., Ed.; International Tin Council and Department of Mineral Resources: Bangkok, Thailand, 1969; pp. 328–339.
61. Heinrich, E.W.; Levinson, A.A. Studies in the mica group; mineralogy of the rose muscovites. *Am. Mineral. J. Earth Planet. Mater.* **1953**, *38*, 25–49.

62. Černý, P.; Teertstra, D.K.; Chapman, R.; Selway, J.B.; Hawthorne, F.C.; Ferreira, K.; Chackowsky, L.E.; Wang, X.J.; Meintzer, R.E. Extreme fractionation and deformation of the leucogranite–pegmatite suite at Red Cross Lake, Manitoba, Canada. IV. Mineralogy. *Can. Mineral.* **2012**, *50*, 1839–1875. [[CrossRef](#)]
63. Smeds, S.A. Zoning and fractionation trends of a peraluminous NYF granitic pegmatite field at Falun, south-central Sweden. *Gff* **1994**, *116*, 175–184. [[CrossRef](#)]
64. Paul, B.J. Mineralogy and Petrochemistry of the Huron Claim Pegmatite, Southeastern Manitoba. Master's Thesis, University of Manitoba, Winnipeg, MB, Canada, 2013.
65. Marciano, V.R.P.D.R. O Distrito Pegmatítico de Santa Maria de Itabira, MG: Mineralogia, Geoquímica e Zoneografia. Ph.D. Thesis, Universidade de São Paulo, São Paulo, Brazil, 1995.
66. Bonzi, W.M.E.; Van Lichtervelde, M.; Vanderhaeghe, O.; André-Mayer, A.S.; Salvi, S.; Wenmenga, U. Insights from mineral trace chemistry on the origin of NYF and mixed LCT+ NYF pegmatites and their mineralization at Mangodara, SW Burkina Faso. *Miner. Depos.* **2023**, *58*, 75–104. [[CrossRef](#)]
67. Faria, P. The Mineralogy and Chemistry of the Spro Pegmatite Mine, Nesodden, and Their Genetic Implications. Master's Thesis, University of Oslo, Oslo, Norway, 2019.
68. Rosing-Schow, N.; Müller, A.; Friis, H. A comparison of the mica geochemistry of the pegmatite fields in southern Norway. *Can. Mineral.* **2018**, *56*, 463–488. [[CrossRef](#)]
69. Manuylova, M.M.; Petrov, L.L.; Rybakova, M.M.; Sokolov, Y.M.; Shmakin, B.M. Distribution of alkali-metals and beryllium in pegmatite minerals from the north Baykalian pegmatite belt. *Geochem. Int.* **1966**, *3*, 309–321.
70. Schuster, R.; Knoll, T.; Mali, H.; Huet, B.; Griesmeier, G.E.U. Field trip guide: A profile from migmatites to spodumene pegmatites (Styria, Austria). *Berichte Geol. Bundesanst.* **2019**, *134*, 1–4.
71. Knoll, T.; Huet, B.; Schuster, R.; Mali, H.; Ntaflos, T.; Hauzenberger, C. Lithium pegmatite of anatectic origin—A case study from the Austroalpine Unit Pegmatite Province (Eastern European Alps): Geological data and geochemical model. *Ore Geol. Rev.* **2023**, *154*, 105298. [[CrossRef](#)]
72. Harmon, R.S.; Lawley, C.J.; Watts, J.; Harraden, C.L.; Somers, A.M.; Hark, R.R. Laser-induced breakdown spectroscopy—An emerging analytical tool for mineral exploration. *Minerals* **2019**, *9*, 718. [[CrossRef](#)]
73. Lawley, C.J.; Somers, A.M.; Kjarsgaard, B.A. Rapid geochemical imaging of rocks and minerals with handheld laser induced breakdown spectroscopy (LIBS). *J. Geochem. Explor.* **2021**, *222*, 106694. [[CrossRef](#)]
74. Fabre, C.; Ourti, N.E.; Ballouard, C.; Mercadier, J.; Cauzid, J. Handheld LIBS analysis for in situ quantification of Li and detection of the trace elements (Be, Rb and Cs). *J. Geochem. Explor.* **2022**, *236*, 106979. [[CrossRef](#)]
75. Wise, M.A.; Francis, C.A. Distribution, classification and geological setting of granitic pegmatites in Maine. *Northeast. Geol.* **1992**, *14*, 82–93.
76. Wise, M.A.; Brown, C.D. Mineral chemistry, petrology and geochemistry of the Sebago granite-pegmatite system, southern Maine, USA. *J. Geosci.* **2010**, *55*, 3–26. [[CrossRef](#)]

Disclaimer/Publisher's Note: The statements, opinions and data contained in all publications are solely those of the individual author(s) and contributor(s) and not of MDPI and/or the editor(s). MDPI and/or the editor(s) disclaim responsibility for any injury to people or property resulting from any ideas, methods, instructions or products referred to in the content.